

Mamoru Minami¹

Professor
Graduate School of Natural
Science and Technology,
Okayama University,
Okayama,
Okayama 700-8530, Japan
e-mail: minami-m@cc.okayama-u.ac.jp

Xiang Li

Graduate School of Natural
Science and Technology,
Okayama University,
Okayama,
Okayama 700-8530, Japan

Takayuki Matsuno

Graduate School of Natural
Science and Technology,
Okayama University,
Okayama,
Okayama 700-8530, Japan
e-mail: matsuno@cc.okayama-u.ac.jp

Akira Yanou

Associate Professor
Department of Radiological Technology,
Kawasaki College of Allied
Health Professions,
Kurashiki,
Okayama 701-0194, Japan
e-mail: yanou-a@mw.kawasaki-m.ac.jp

Dynamic Reconfiguration Manipulability for Redundant Manipulators

This paper analyzes the dynamics of robotic manipulator based on a concept called dynamic reconfiguration manipulability (DRM), which gauges the dynamical shape-changeability of a robot based on the redundancy of the robot and the premise that the primary task is the hand task. DRM represents how much acceleration each intermediate link can generate and in what direction the acceleration can be realized based on normalized torque inputs. This concept will aid in the optimization of the design and control of robots. The appropriateness and usefulness of DRM were confirmed by applying it to redundant manipulators and comparing it with the known concept of avoidance manipulability. [DOI: 10.1115/1.4033667]

1 Introduction

In the field of robotic manipulation, studies conducted since the 1980s have considered indices that indicate the motion capability of a manipulator's hand from the perspective of kinematics and dynamics with the objectives of determining the ability of a manipulator to perform certain tasks and designing a new manipulator. A generalized inertia ellipsoid that indicates the relationship between an external force applied to a hand and the acceleration of the hand was proposed by Asada [1]. Yoshikawa [2] proposed a measure of manipulability that indicates the relationship between the joint angular velocity and the hand velocity based on the nature of the Jacobian matrix from the perspective of kinematics.

Additional related concepts that have been proposed in previous studies are as follows. Dynamic manipulability [3–5] indicates the relationship between the acceleration of the hand and the joint torque considering constraints imposed by the equations of motion from the perspective of dynamics. This measure of manipulability is visualized as an ellipsoid that expresses which direction in Cartesian coordinate space a robot's hand will accelerate given a unit input torque. Furthermore, the singularity of the manipulator has been discussed with regard to these measures of manipulability. Recently, Kurazume et al. proposed an index called the impedance matching ellipsoid, which expresses a unified explanation of both dynamic manipulability and the manipulating force ellipsoid [6]. Additionally, an extended manipulability measure for a biarticular driving joint was discussed by Yoshida et al. [7]. The zero moment point manipulability ellipsoid was proposed by Naksuk

and Lee [8] to describe bipedal robots. Such manipulability indices have been continuously discussed for the purposes of explaining robot motion with scalar values and applying the indices to robot control.

In recent decades, there have been discussions on reconfigurable robots, which have structures whose components can be separated and reconstructed in different shapes to enable the robot to execute a task different from the task or tasks that could be performed in the previous configuration. The word “reconfiguration” has been used frequently in this sphere of robotic research [9–11].

Conversely, the shape-changeability of serial-link redundant manipulators with primary tasks related to hand motion has also been discussed by using a word reconfiguration [12–15]. This concept has been extended to a mobile robot with kinematical redundancies traveling on uneven terrain [16]. Thus, there have been two concepts concerning reconfiguration, one in Refs. [9–11] and the others above, then in this paper we use reconfiguration for shape-changeability of serial-link redundant manipulators as in Refs. [12–17].

The concept of DRM is proposed in Refs. [14] and [17] in light of the shape-changeability mentioned above. The originality and efficiency of the proposed concept lay in the reconfigurable accelerations of intermediate links, which are evaluated through both dynamical equations of motion and kinematical aspects. DRM represents the degree of realizable acceleration at intermediate links to which the structure and shape of a manipulator can be reconfigured on the condition that the acceleration of a hand task is prioritized, thus indicating the produceable acceleration response performance for reconfiguration of a redundant manipulator.

Researchers have debated how to utilize redundancy to define predetermined criteria that can be used as yardsticks for

¹Corresponding author.

Manuscript received July 30, 2015; final manuscript received May 6, 2016; published online September 6, 2016. Assoc. Editor: Leila Notash.

optimizing the performance of the robot control. The criteria are specified based on the demand specifications of the robots' required tasks and thus tend to be task-dependent [18–20]. Therefore, these criteria are not used for general purposes, such as redesigning the mechanism and structure of a robot. The main theories concerning the control methods used to optimize criteria through the redundancy of robots have been compiled in Ref. [21]. These achievements concerning optimal control are not in line with the objective of evaluating the structures and shapes of manipulators and not aimed at the ultimate goal of redesigning the structure of the robot. This demonstrates the clear difference between studies on the control method [18–21] and the concept of DRM proposed in Refs. [14] and [17], and the DRM is extended in this paper.

In contrast, avoidance manipulability represents the extent to which the velocity of intermediate links can be produced by the normalized unit angular velocities of joints for the purpose of changing the shape of the manipulator, given that the hand velocity is prioritized [12,13,22]. The consideration of the shape of the manipulator is then based purely on the kinematical relations between the realizable velocities of intermediate links and the angular velocities of the joints. Furthermore, the effectiveness of the manipulator in avoiding both hindering objects and singularities has been confirmed. Avoidance manipulability is, however, a concept based on the velocity capabilities of intermediate links rather than their acceleration capabilities. This is a kinematical consideration of velocity without dynamics. Therefore, there are cases where avoidance manipulability based on kinematics is not effective, such that the effects of dynamics become dominant when discussing generable acceleration.

Because this paper is based on results we obtained in a previous study, the concept of dynamic manipulability given in Sec. 2 of this paper is similar to that presented in our previous studies [14,17]. However, Sec. 3 of this paper, which includes the analysis of DRM in the case of a hand oscillatory acceleration task being given as the primary task, reveals the difference between the DRM ellipsoid (DRME) and the reconfiguration manipulability (RM) ellipsoid, emphasizing that the kinematical and dynamical manipulabilities differ and should be discussed separately depending on the hand and intermediate link tasks, which was not discussed in our previous studies [14,17]. Furthermore, this paper reveals that the optimal configurations of the manipulator evaluated by the DRM and RM ellipsoids (RMEs) are different, which suggests that whether DRM or RM should be used to optimize the entire configuration of the manipulator hinges on what type of task is required for the hand and intermediate links.

This paper proposes the concept of DRM as a measure of how much acceleration a dynamical system can produce in a workspace with a normalized input torque. This new measure represents the extent to which the dynamical system of a robot is capable of producing shape-reconfigurable acceleration in a workspace with a unit torque input for all the joints while executing primary hand tasks. Furthermore, the effectiveness of using DRM for design and configuration optimization and the physical properties of DRM were investigated in this study. The effectiveness of using DRM was confirmed through simulations in which a redundant manipulator was adopted, and the possibility of using DRM to measure the capabilities of a humanoid robot while performing a walking task is discussed.

2 DRM

2.1 Dynamic Manipulability. In general, the dynamical equation for a serial-link manipulator is given as

$$M(q)\ddot{q} + h(q, \dot{q}) + g(q) + D\dot{q} = \tau \quad (1)$$

where $M(q) \in \mathbb{R}^{n \times n}$ is the inertia matrix; $h(q, \dot{q}) \in \mathbb{R}^n$ and $g(q) \in \mathbb{R}^n$ are the Coriolis force, centrifugal force, and gravity vectors, respectively; $D = \text{diag}[d_1, d_2, \dots, d_n]$ is a matrix

containing the coefficients of the viscous friction of the joints; and $\tau \in \mathbb{R}^n$ is the joint torque. The kinematic equation of a robot describes the relationship between the position $r_i \in \mathbb{R}^m$ of the i th link in Cartesian space and the joint angle $q \in \mathbb{R}^n$ and is given by

$$r_i = f_i(q) \quad (i = 1, 2, \dots, n) \quad (2)$$

Differentiating Eq. (2) yields

$$\dot{r}_i = J_i \dot{q} \quad (i = 1, 2, \dots, n) \quad (3)$$

where $J_i \in \mathbb{R}^{m \times n}$ is a Jacobian matrix with the zero block matrix $J_i = [J_i, 0]$. Differentiating Eq. (3) yields

$$\ddot{r}_i = J_i(q)\ddot{q} + \dot{J}_i(q)\dot{q} \quad (4)$$

Then, Eqs. (1) and (4) yield the following equation:

$$\ddot{r}_i - \dot{J}_i(q)\dot{q} = J_i M^{-1}[\tau - h(q, \dot{q}) - g(q) - D\dot{q}] \quad (5)$$

Here, the two new variables, $\tilde{\tau}$ and \ddot{r}_i , are defined as

$$\tilde{\tau} \triangleq \tau - h(q, \dot{q}) - g(q) - D\dot{q} \quad (6)$$

$$\ddot{r}_i \triangleq \ddot{r}_i - \dot{J}_i(q)\dot{q} \quad (7)$$

Thus, Eq. (5) can be rewritten as

$$\ddot{r}_i = J_i M^{-1} \tilde{\tau} \quad (i = 1, 2, \dots, n) \quad (8)$$

Dynamic manipulability is an index that represents the ease with which the acceleration of each link can be generated by the joint torque. Equation (8) is the basis of dynamic manipulability, and its general solution can be expressed as

$$\tilde{\tau} = (J_i M^{-1})^+ \ddot{r}_i + [I_n - (J_i M^{-1})^+ (J_i M^{-1})]k \quad (9)$$

where $(J_i M^{-1})^+$ is the quasi-inverse matrix of $(J_i M^{-1})$, $I_n \in \mathbb{R}^{n \times n}$ is a unit matrix, and $k \in \mathbb{R}^n$ is an arbitrary vector.

Next, the set of \ddot{r}_i yielded by all the joint torques $\tilde{\tau}$ that satisfies the Euclidean norm condition $\|\tilde{\tau}\| = (\tilde{\tau}_1^2 + \tilde{\tau}_2^2 + \dots + \tilde{\tau}_n^2)^{1/2} \leq 1$ is expressed as

$$\ddot{r}_i^T [J_i (M^T M)^{-1} J_i^T]^+ \ddot{r}_i \leq 1 \quad (10)$$

where $\ddot{r}_i \in \mathbb{R}(J_i M^{-1})$ must be satisfied, and $\mathbb{R}(J_i M^{-1})$ represents a space that has the same dimension as the range of $J_i M^{-1}$. Thus, the set produces an ellipsoid in a space that has the same dimension as the range of $J_i M^{-1}$. The ellipsoid of each link described by Eq. (10) is called the dynamic manipulability ellipsoid (DME) [3] (Fig. 1(a)).

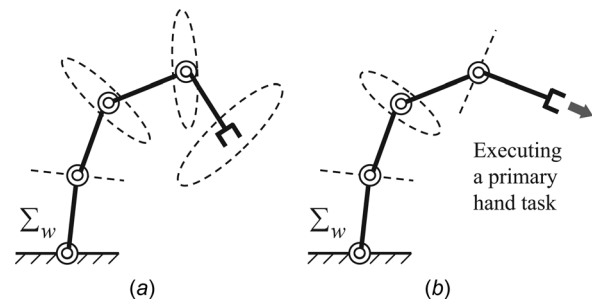


Fig. 1 (a) DMEs represent the possible accelerations of all the links with no prioritized task. (b) DRMEs represent the possible accelerations of intermediate links while the system is executing the primary task.

2.2 DRM. In this study, the acceleration $\ddot{\mathbf{r}}_{nd}$ of the hand is assumed to be the primary task. The relationship between $\ddot{\mathbf{r}}_n$ and $\tilde{\boldsymbol{\tau}}$ is obtained by substituting n for i in Eq. (8)

$$\ddot{\mathbf{r}}_n = \mathbf{J}_n \mathbf{M}^{-1} \tilde{\boldsymbol{\tau}} \quad (11)$$

By calculating the general solution of Eq. (11), the torque $\tilde{\boldsymbol{\tau}}$ that can realize the desired acceleration $\ddot{\mathbf{r}}_{nd}$ can be obtained as

$$\tilde{\boldsymbol{\tau}} = (\mathbf{J}_n \mathbf{M}^{-1})^+ \ddot{\mathbf{r}}_{nd} + [\mathbf{I}_n - (\mathbf{J}_n \mathbf{M}^{-1})^+ (\mathbf{J}_n \mathbf{M}^{-1})] \mathbf{l} \quad (12)$$

where \mathbf{l} is an arbitrary vector satisfying $\mathbf{l} \in \mathbb{R}^n$. The leading superscript of “1” in \mathbf{l} indicates the first dynamic reconfiguration task. The first term on the right-hand side of Eq. (12) denotes the solution that minimizes $\tilde{\boldsymbol{\tau}}$ in the null space of $\mathbf{J}_n \mathbf{M}^{-1}$ when implementing $\ddot{\mathbf{r}}_{nd}$. The second term on the right-hand side of Eq. (12) means that \mathbf{l} gives the joint torque vector that can change the configuration of manipulator independently of the hand acceleration for the purpose of tracking the desired trajectory.

Next, the DRM of the j th middle link ($1 \leq j \leq n-1$) was considered. The task that is subordinate to the primary hand task is called the “first dynamic reconfiguration task.” As stated above, variables related to this task are denoted by a leading superscript of “1,” indicating that the task is the first priority in the overall reconfiguration task. If the redundancy of the manipulator is sufficiently high, it is possible to execute the second and third reconfiguration tasks.

The relationship between $\ddot{\mathbf{r}}_{nd}$, which is the desired hand acceleration, and ${}^1\ddot{\mathbf{r}}_j$, which is the acceleration of the j th link, can be expressed by combining Eqs. (8) and (12) and eliminating $\tilde{\boldsymbol{\tau}}$ as

$${}^1\ddot{\mathbf{r}}_j = \mathbf{J}_j \mathbf{M}^{-1} (\mathbf{J}_n \mathbf{M}^{-1})^+ \ddot{\mathbf{r}}_{nd} + \mathbf{J}_j \mathbf{M}^{-1} [\mathbf{I}_n - (\mathbf{J}_n \mathbf{M}^{-1})^+ (\mathbf{J}_n \mathbf{M}^{-1})] \mathbf{l} \quad (13)$$

According to Eq. (7), Eq. (13) can then be rewritten as

$$\begin{aligned} {}^1\ddot{\mathbf{r}}_j - \dot{\mathbf{J}}_j \dot{\mathbf{q}} - \mathbf{J}_j \mathbf{M}^{-1} (\mathbf{J}_n \mathbf{M}^{-1})^+ (\ddot{\mathbf{r}}_{nd} - \dot{\mathbf{J}}_n \dot{\mathbf{q}}) \\ = \mathbf{J}_j \mathbf{M}^{-1} [\mathbf{I}_n - (\mathbf{J}_n \mathbf{M}^{-1})^+ (\mathbf{J}_n \mathbf{M}^{-1})] \mathbf{l} \end{aligned} \quad (14)$$

Here, the three new variables, ${}^1\ddot{\mathbf{r}}_j$, $\Delta {}^1\ddot{\mathbf{r}}_j$, and ${}^1\boldsymbol{\Lambda}_j$, are defined as

$${}^1\ddot{\mathbf{r}}_j \triangleq \dot{\mathbf{J}}_j \dot{\mathbf{q}} + \mathbf{J}_j \mathbf{M}^{-1} (\mathbf{J}_n \mathbf{M}^{-1})^+ (\ddot{\mathbf{r}}_{nd} - \dot{\mathbf{J}}_n \dot{\mathbf{q}}) \quad (15)$$

$$\Delta {}^1\ddot{\mathbf{r}}_j \triangleq {}^1\ddot{\mathbf{r}}_j - {}^1\ddot{\mathbf{r}}_j, \quad (16)$$

$${}^1\boldsymbol{\Lambda}_j \triangleq \mathbf{J}_j \mathbf{M}^{-1} [\mathbf{I}_n - (\mathbf{J}_n \mathbf{M}^{-1})^+ (\mathbf{J}_n \mathbf{M}^{-1})] \quad (17)$$

Equation (14) can then be rewritten as

$$\Delta {}^1\ddot{\mathbf{r}}_j = {}^1\boldsymbol{\Lambda}_j \mathbf{l} \quad (18)$$

The relationship between $\ddot{\mathbf{r}}_{nd}$, $\ddot{\mathbf{r}}_{nd}$, ${}^1\ddot{\mathbf{r}}_j$, and $\Delta {}^1\ddot{\mathbf{r}}_j$ is shown in Fig. 2. The secondary goal of the manipulator is to generate the acceleration $\ddot{\mathbf{r}}_{nd}$ to ensure the completion of the hand task $\ddot{\mathbf{r}}_{nd}$

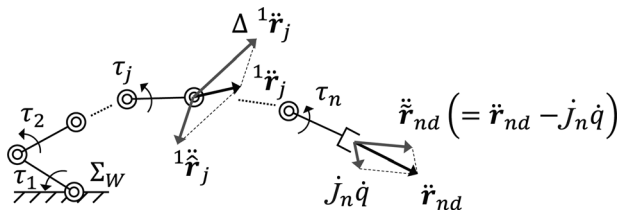


Fig. 2 Reconfiguration at intermediate link while executing hand task

despite the influence of the acceleration $\dot{\mathbf{J}}\dot{\mathbf{q}}$. In Eq. (15), ${}^1\ddot{\mathbf{r}}_j$ represents the acceleration caused by the configuration of the shape of the manipulator. The first term on the right-hand side of Eq. (15) denotes the Coriolis and centrifugal acceleration of the j th link, and the second term represents the acceleration of the j th link, which is generated to realize the hand task. From Eq. (16), it is clear that in order to realize ${}^1\ddot{\mathbf{r}}_j$ independently of $\Delta {}^1\ddot{\mathbf{r}}_j$, $\Delta {}^1\ddot{\mathbf{r}}_j$ should be generated by utilizing ${}^1\mathbf{l}$, which is a part of the input torque. Based on Eq. (18), DRM is proposed as an index to indicate the ease with which the acceleration of a middle link can be generated by a torque ${}^1\mathbf{l}$ that has no influence on the desired acceleration $\ddot{\mathbf{r}}_{nd}$ of the hand. However, it is unclear whether a feasible value of the acceleration ${}^1\ddot{\mathbf{r}}_j$ can be yielded through $\Delta {}^1\ddot{\mathbf{r}}_j \in \mathbb{R}^m$, which is an issue of concern. This acceleration depends on ${}^1\boldsymbol{\Lambda}_j$; thus, the possibility of realizing ${}^1\ddot{\mathbf{r}}_j$ can be judged by analyzing ${}^1\boldsymbol{\Lambda}_j$. The general solution ${}^1\mathbf{l}$ to Eq. (18), which realizes ${}^1\ddot{\mathbf{r}}_j$, can be obtained as

$${}^1\mathbf{l} = {}^1\boldsymbol{\Lambda}_j^+ \Delta {}^1\ddot{\mathbf{r}}_{jd} + (\mathbf{I}_n - {}^1\boldsymbol{\Lambda}_j^+ {}^1\boldsymbol{\Lambda}_j) {}^2\mathbf{l} \quad (19)$$

where ${}^2\mathbf{l}$ is a new arbitrary vector that satisfies ${}^1\mathbf{l} \in \mathbb{R}^n$. If $\text{rank}(\mathbf{I}_n - {}^1\boldsymbol{\Lambda}_j^+ {}^1\boldsymbol{\Lambda}_j) \geq 1$, all the middle links except the j th link are capable of generating the desired acceleration. Assuming the constraint condition $\|{}^1\mathbf{l}\| \leq 1$ yields the inequality

$$(\Delta {}^1\ddot{\mathbf{r}}_{jd})^T ({}^1\boldsymbol{\Lambda}_j^+)^T {}^1\boldsymbol{\Lambda}_j^+ \Delta {}^1\ddot{\mathbf{r}}_{jd} \leq 1 \quad (20)$$

If $\text{rank}({}^1\boldsymbol{\Lambda}_j) = m$, Eq. (20) represents an ellipsoid expanding in an m -dimensional space. Furthermore, when $\text{rank}({}^1\boldsymbol{\Lambda}_j) < m$, the solution of Eq. (20) is a degenerate ellipsoid, as shown in Fig. 1(b).

Next, an index to compare the configuration of the manipulator based on the concept of DRM is considered. Applying the singular value decomposition to the matrix $\boldsymbol{\Lambda}$ yields

$${}^1\boldsymbol{\Lambda}_j = {}^1\mathbf{U}_j {}^1\boldsymbol{\Sigma}_j {}^1\mathbf{V}_j^T \quad (21)$$

$${}^1\boldsymbol{\Sigma}_j = \begin{matrix} r & n-r \\ \begin{pmatrix} {}^1\sigma_{j,1} & 0 & \\ & \ddots & 0 \\ 0 & & {}^1\sigma_{j,r} \\ & 0 & 0 \end{pmatrix} \end{matrix} \quad (22)$$

where ${}^1\mathbf{U} \in \mathbb{R}^{m \times m}$ and ${}^1\mathbf{V} \in \mathbb{R}^{n \times n}$ are the orthogonal matrixes, r denotes the number of nonzero singular values of ${}^1\boldsymbol{\Lambda}_j$, and $\sigma_{j,1} \geq \dots \geq \sigma_{j,r} > 0$. In addition, $r \leq m$ because $\text{rank}({}^1\boldsymbol{\Lambda}_j) \leq m$. Thus, when a hand task is given, the dynamic reconfiguration capability of the j th link can be described by

$${}^1w_j = {}^1\sigma_{j,1} {}^1\sigma_{j,2} \dots {}^1\sigma_{j,r} \quad (23)$$

In this paper, w_j in Eq. (23) is defined as the dynamic reconfiguration manipulability measure (DRMM), which indicates how much acceleration can be generated at the tip of the j th link in an arbitrary direction.

Here, it should be noted that both the DRME and the DRMM are determined by ${}^1\boldsymbol{\Lambda}_j$. In addition, ${}^1\boldsymbol{\Lambda}_j$ is a function of $\mathbf{J}_i(\mathbf{q})$, $\mathbf{J}_n(\mathbf{q})$, and $\mathbf{M}(\mathbf{q})$, as indicated in Eq. (17). Finally, ${}^1\boldsymbol{\Lambda}_j$ is dependent on \mathbf{q} but not $\dot{\mathbf{q}}$. Therefore, both the DRME and the DRMM are determined by the current configuration of the manipulator and not by the reconfiguration velocity.

2.3 Comparison of DRM and RM. A previous study proposed the concept of avoidance manipulability as an index of the

redundancy of a manipulator [22]. Avoidance manipulability was constructed from the perspective of kinematics and thus does not include the influences of dynamic properties, such as mass and inertia. This section discusses the difference between DRM and avoidance manipulability. For the sake of clarity, avoidance manipulability is hereafter referred to as reconfiguration manipulability [12,13].

A measure of RM can be obtained as follows: First, substituting n for i in Eq. (3) yields

$$\dot{r}_n = J_n \dot{q} \quad (24)$$

Next, the general solution \dot{q} of Eq. (24) is calculated as

$$\dot{q} = J_n^+ \dot{r}_{nd} + (I_n - J_n^+ J_n)^+ l_q \quad (25)$$

where $l_q \in \mathbb{R}^n$ is an arbitrary vector. Then, the velocity ${}^1\dot{r}_j$ of the j th middle link is obtained as a function of the desired velocity ${}^1\dot{r}_{nd}$ of the hand, as

$${}^1\dot{r}_j = J_j J_n^+ \dot{r}_{nd} + J_j (I_n - J_n^+ J_n)^+ l_q \quad (26)$$

Redefining the variables in Eq. (26) as

$$\Delta^1 \dot{r}_j \triangleq \dot{r}_j - J_j J_n^+ \dot{r}_{nd} \quad (27)$$

$${}^1 J_{Qj} \triangleq J_j (I_n - J_n^+ J_n) \quad (28)$$

yields

$$\Delta^1 \dot{r}_j = {}^1 J_{Qj} l_q \quad (29)$$

The set of velocities that can be generated at the tip of the j th link is defined as the RME under the constraint $\|l_q\| \leq 1$ given in Eq. (29). The RME is expressed as

$$(\Delta^1 \dot{r}_j)^T ({}^1 J_{Qj} {}^1 J_{Qj}^T)^+ \Delta^1 \dot{r}_j \leq 1 \quad (30)$$

The RM measure (RMM), which indicates the ease with which the velocity of the middle link can be generated, is derived from Eq. (30) [13].

3 Application of DRM to Four-Link Manipulator

To confirm its physical properties, DRM was adopted to analyze a four-link planar manipulator placed in the yz -plane, as shown in Fig. 3. Additionally, simulations were performed to

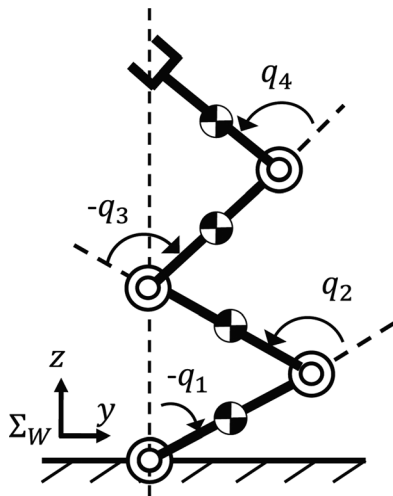


Fig. 3 Four-link manipulator

verify the effectiveness of the indices based on DRM. Each link of the manipulator had a weight of 1.0 kg and a length of 0.3 m in the simulation, and the center of gravity of each link was assumed to be at its center. The coefficient of viscous friction of each joint was set to 1.0 N·m/(rad s).

3.1 Properties of DRM. The manipulability of the second joint of the four-link manipulator was investigated under the condition that the third joint and the hand always exist on a vertical line that passes through the first joint, as shown by the dotted line in Fig. 3. The DRM of a manipulator is determined according to its configuration, and the configuration of the four-link manipulator considered in this study was determined from the angles of the joints. In this case, however, the joint angles were constrained by the two abovementioned conditions placed on the third joint and the hand. Thus, the number of independent variables was reduced to two parameters; for example, q_2 and q_4 can be set as independent variables with q_1 and q_3 defined as functions of q_2 and q_4 , as $q_1 = -q_2/2$ and $q_3 = -(q_2 + q_4)/2$.

3.1.1 Example of DRM Calculation. The joint angles were set as $q_1 = -45$ deg, $q_2 = 90$ deg, $q_3 = -90$ deg, and $q_4 = 90$ deg. In this case, the configuration of the manipulator and the DRME of the tip of the second link were defined as in Fig. 4. The DRME depends on both the selection of the desired acceleration of the hand, which determines $\Delta^1 \dot{r}_j$ through ${}^1 \ddot{r}_j$ in Eqs. (15) and (16), and the structure and/or configuration of the manipulator. The input torque was calculated as

$$\tau = u + (J_4 M^{-1})^+ \ddot{r}_{4d} + [I_4 - (J_4 M^{-1})^+ (J_4 M^{-1})] l \quad (31)$$

where $u = h + g + D\dot{q}$. First, the desired acceleration of the hand was given as $\ddot{r}_{4d} = [a_{4y}, a_{4z}]^T = [0, 0]^T$, and \dot{q} was set to zero. Under these conditions, based on Eq. (7), $\ddot{r}_i = \ddot{r}_i$ must be satisfied. Figure 5 shows the results of a simulation when random values of $\|l\| \leq 1$ were input with the prioritized task $\ddot{r}_{nd} = [0, 0]^T$. In Fig. 5(a), the ellipse drawn with a solid line represents the DRME calculated from Eq. (20). Additionally, the markers in Fig. 5(a) express accelerations $\Delta^1 \ddot{r}_2$ that were randomly selected and satisfy Eq. (18) with the condition $\|l\| \leq 1$. Because the desired acceleration of the hand is $\ddot{r}_{4d} = 0$, the region encompassing the possible values of the acceleration generated to change the position of the tip of the second link without influencing the acceleration of the hand was investigated based on the DRME. Figure 5(a) demonstrates that the possible values of $\Delta^1 \ddot{r}_2$ generated under the condition $\|l\| \leq 1$ fall within the DRME ellipse. The origin of the coordinate systems in Figs. 5 and 6 corresponds to the tip of the second link in Fig. 4. Additionally, the y - and z -axes of these coordinate systems match the y - and z -axes of the coordinate system Σ_W in Fig. 4. From the constraint conditions $\ddot{r}_{4d} = 0$ and

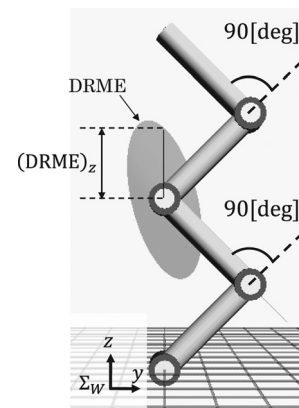


Fig. 4 Configuration of manipulator

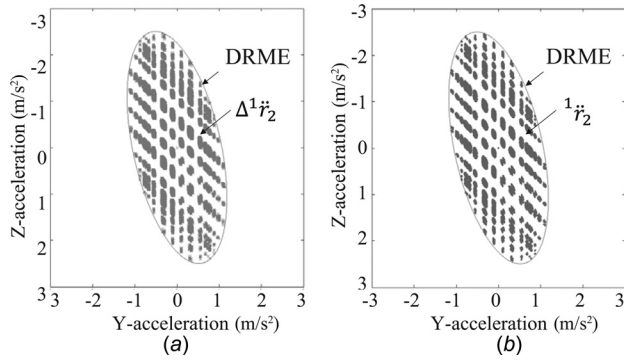


Fig. 5 Results of the simulation when the random values of $\|{}^1\dot{r}_i\| \leq 1$ are input with the prioritized task $\ddot{r}_{nd} = [0, 0]^T$: (a) $\Delta^1\ddot{r}_2$ and (b) ${}^1\ddot{r}_2$

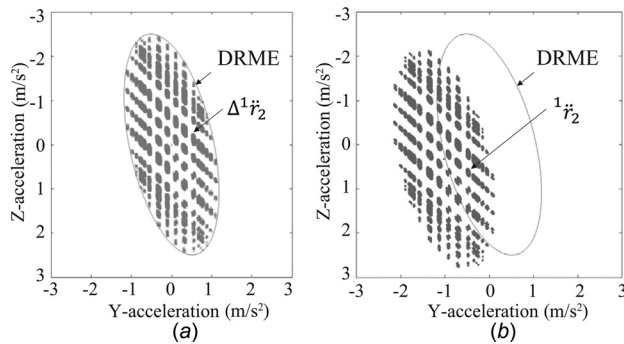


Fig. 6 Results of the simulation when the random values of $\|{}^1\dot{r}_i\| \leq 1$ are input with the prioritized task $\ddot{r}_{nd} = [1, 0]^T$: (a) $\Delta^1\ddot{r}_2$ and (b) ${}^1\ddot{r}_2$

$\dot{q} = 0$, ${}^1\ddot{r}_j = 0$ can be derived from Eq. (13), and $\Delta^1\ddot{r}_2 = {}^1\ddot{r}_2$ can be derived from Eq. (14). To confirm these derivations, the distribution of \ddot{r}_2 was plotted, as shown in Fig. 5(b). Substituting the joint torque τ calculated from Eq. (31) into Eq. (1) yielded \dot{q} , and then, \ddot{r}_2 was obtained by substituting \dot{q} into Eq. (4). Because the reconfiguration acceleration \ddot{r}_2 represents the first reconfiguration acceleration, \ddot{r}_2 is equivalent to ${}^1\ddot{r}_2$ in the current discussion, and these variables are hereafter considered equivalent. It was thus confirmed that $\Delta^1\ddot{r}_2$, which is shown in Fig. 5(a), and ${}^1\ddot{r}_2$, which is shown in Fig. 5(b), are equivalent.

Next, $\Delta^1\ddot{r}_2$ and ${}^1\ddot{r}_2$ were plotted with the conditions ${}^1\ddot{r} \neq 0$ and ${}^1\ddot{r}_{Ad} = [1, 0]^T$ applied to Eq. (15), as shown in Fig. 6. Figures 6(a) and 6(b) illustrate the DRME and distribution of $\Delta^1\ddot{r}_2$ and those of \ddot{r}_2 , respectively. Based on Fig. 6, $\Delta^1\ddot{r}_2$ and \ddot{r}_2 are not equivalent. Because ${}^1\ddot{r}_{Ad} = [1, 0]^T$ was given as a condition, ${}^1\ddot{r}_2 = [-1.02, -0.33]^T$ was generated, and then \ddot{r}_2 moved outside of the DRME, partially as a result of the influence of ${}^1\ddot{r}_2$. This phenomenon was caused by influence of the desired hand acceleration. It is clear from Eq. (16) that ${}^1\ddot{r}_2$ was the acceleration element that was obtained by shifting $\Delta^1\ddot{r}_2$ from the DRME by ${}^1\ddot{r}_2 = [-1.02, -0.33]^T$. In addition, comparing Figs. 5(a) and 6(a) confirms that the DRME is independent of the desired hand acceleration ${}^1\ddot{r}_{Ad}$.

In Figs. 5 and 6, the desired acceleration values are plotted in a disproportionate pattern. It is considered that this disproportionate pattern forms because the generation of random numbers by c++ is not completely uniform and they are not given in Cartesian space but in joint space; thus Eqs. (15)–(17) may influence the pattern of the data points.

3.1.2 Example of DRMM Calculation. The DRMM can be calculated when the desired acceleration ${}^1\ddot{r}_{Ad} = [a_{4y}, a_{4z}]^T$ of the hand is given. In this section, the DRMM is compared with the RMM to clarify the differences between these two indices. DRM depends on the Jacobian matrix ${}^1J_{Qj}$ given in Eq. (28), whereas the DRMM is dominated by ${}^1\Lambda_j$, which is determined by both the

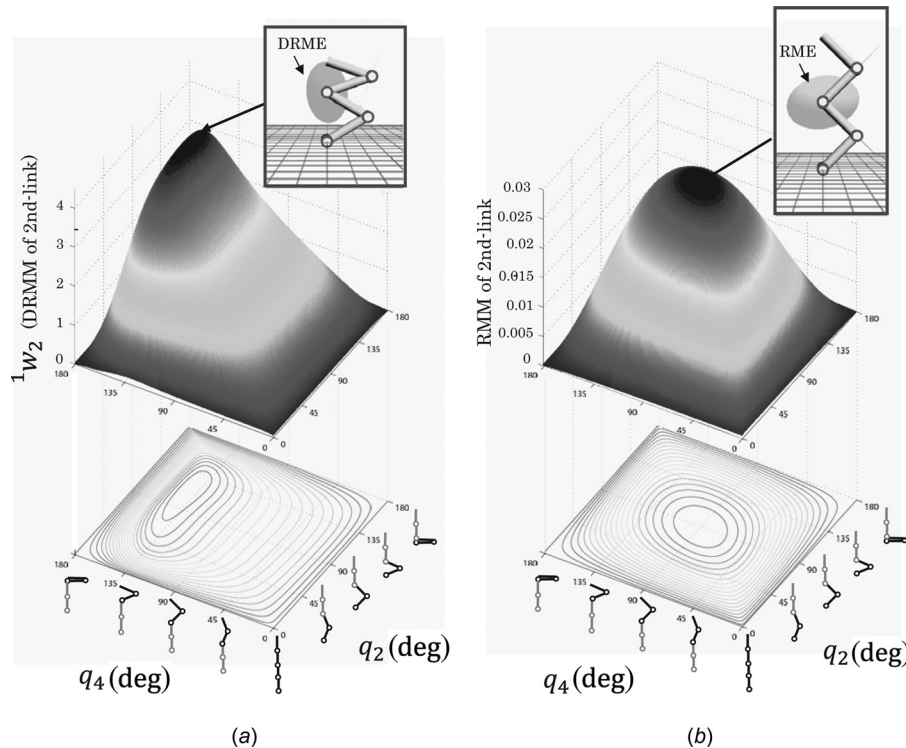


Fig. 7 Maps of (a) DRMM and (b) RMM for four-link manipulator

Jacobian matrix and the inertial matrix. Maps of q_1 and q_2 for the DRMM and RMM are plotted in Figs. 7(a) and 7(b), respectively. The RMM of the second link peaks when $q_2 = 90$ deg and $q_4 = 90$ deg. Additionally, the DRMM peaks when $q_2 = 118$ deg and $q_4 = 141$ deg. The angle of each joint when the DRMM peaks is more acute than that when the RMM peaks. Although the RMM depends on $J_j(q)$ and $J_n(q)$ in Eqs. (27)–(30), the DRMM depends on $J_j(q)$, $J_n(q)$, and $M(q)$.

3.2 Analysis of DRM. The volume of an ellipse formed by the manipulability and an index taken to be in proportion to the volume are used to judge the mobility performance of a manipulator. However, in actual situations, there is an interest in emphasizing the mobility in certain directions. Examples of such preferred directions include the direction of the forward movement of the manipulator hand and the direction of the gravitational force for the waist joint in the case of a bipedal locomotion robot.

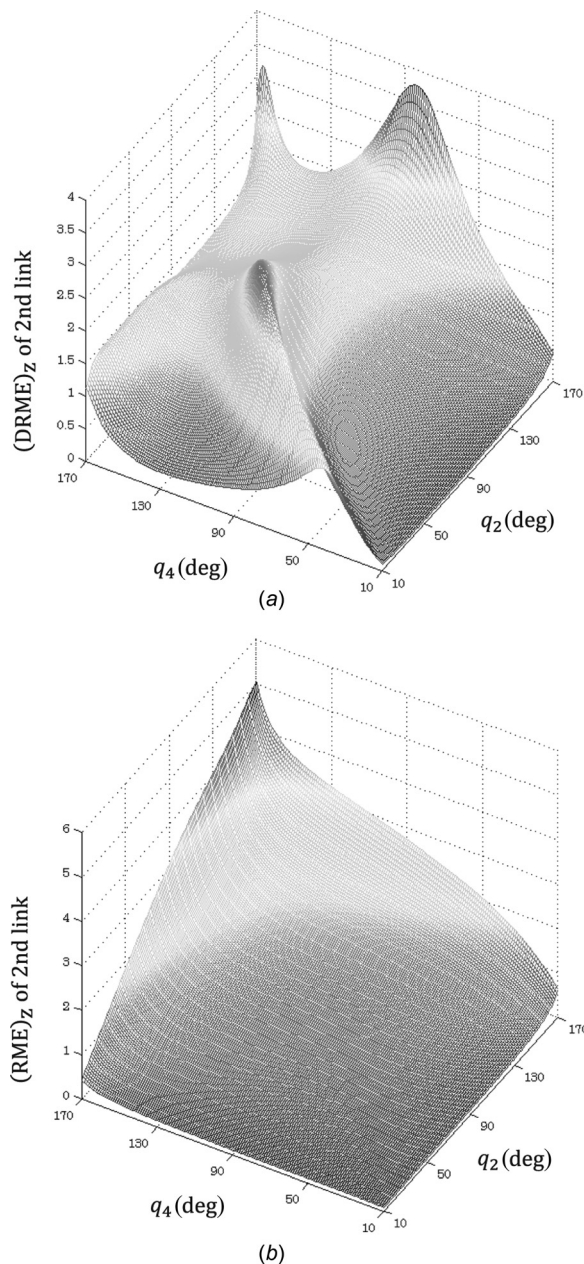


Fig. 8 (a) Vertical acceleration derived from the DRME. (b) Vertical velocity derived from the RME. (a) DRMM and (b) RMM.

Therefore, as shown in Fig. 4, $(DRME)_z$ is defined as a length along the z -direction of the DRME of the second link, and the ease with which the acceleration of the second link of the four-link manipulator can be generated is measured. This measurement involves searching for a configuration that allows jumping behavior if the four-link manipulator is assumed to be a humanoid robot.

$(DRME)_z$ and $(RME)_z$ are plotted in Figs. 8(a) and 8(b), respectively. q_2 and q_4 are arguments of the index maps in Figs. 8(a) and 8(b) in the same manner as in Figs. 7(a) and 7(b). $(RME)_z$ is a monotonically increasing function with respect to q_2 and q_4 , as shown in Fig. 8(b). Conversely, $(DRME)_z$ has a multimodal distribution with respect to q_2 and q_4 , as shown in Fig. 8(a). To understand the detail, cross sections of $(DRME)_z$ and $(RME)_z$ at $q_4 = 130$ deg are plotted in Figs. 9(a) and 9(b), respectively. Additionally, the postures of the robot corresponding to Figs. 9(a) and 9(b) are shown in Figs. 10(a) and 10(b), respectively.

From Fig. 9(b), it is clear that $(RME)_z$ monotonically increases with increasing q_2 ; however, $(DRME)_z$ peaks at $q_2 = 80$ deg. After this peak, $(DRME)_z$ decreases and then increases again as q_2 increases. Two peaks occur at approximately $q_2 = 80$ deg and 170 deg in Fig. 9(a), and the corresponding postures of the manipulator are illustrated in Fig. 10(a). The DRME is dominated by ${}^1\Lambda_j$, which is defined as ${}^1\Lambda_j = J_j M^{-1} [I_n - (J_n M^{-1})^+ (J_n M^{-1})]$. Conversely, the RME is dominated by ${}^1J_{Qj}$, which is defined as ${}^1J_{Qj} = J_j (I_n - J_n^+ J_n)$. The graphs in both Figs. 9(a) and 9(b) have peaks at approximately $q_2 = 170$ deg. J_j and J_n are considered to be among the factors causing these peaks because the DRME and RME are related to J_j and J_n , respectively. Therefore, the peak in the DRME at approximately $q_2 = 80$ deg shown in Fig. 9(a) is considered to be caused by the inertial matrix $M(q)$, which is included in the DRME but not the RME.

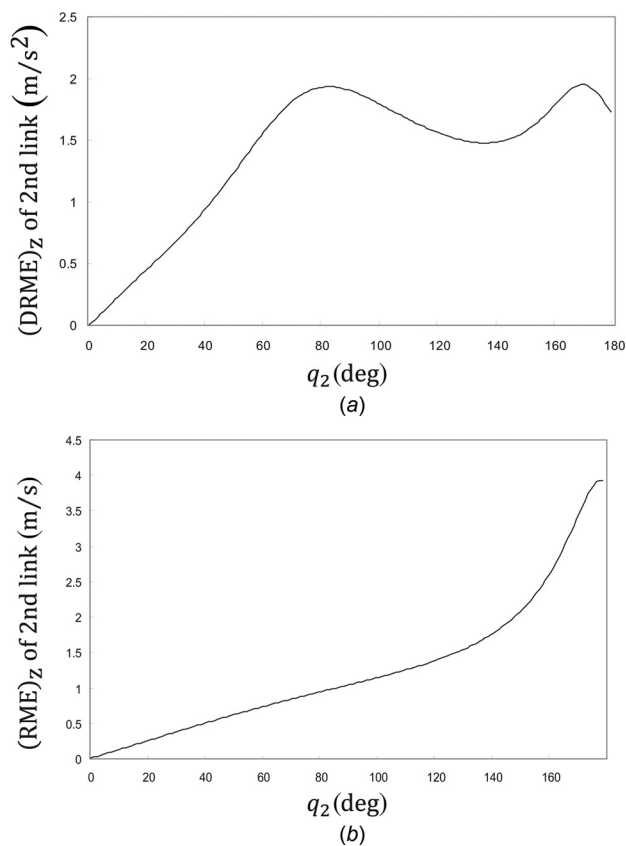


Fig. 9 Vertical acceleration and vertical velocity plotted against q_2 with $q_4 = 130$ deg: (a) vertical acceleration derived from the DRME and (b) vertical velocity derived from the RME

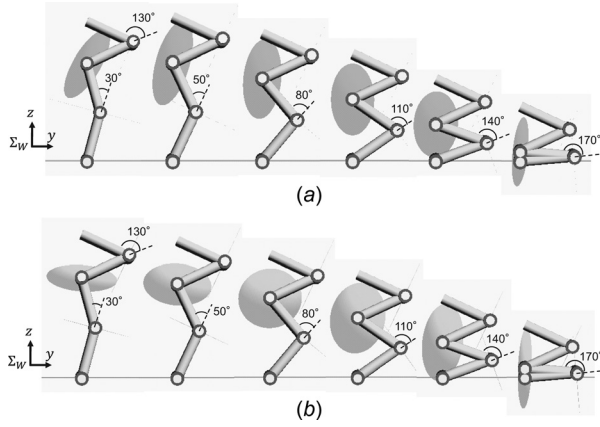


Fig. 10 DRME and RME for various configurations obtained by varying q_2 from 30 deg to 170 deg: (a) DRME and (b) RME

3.3 Realization of Hand Acceleration and Manipulator Posture. It is clear that $\text{rank}({}^1\Lambda_2) = 2$ for the posture shown in Fig. 4 because the DRME of the second link expands in the yz -plane. This means that the accelerations of the hand and the second link can be generated individually on the yz plane. To confirm the capability, the behavior of the manipulator is shown in the case where the periodic acceleration of the hand and the second link are given by the following equations:

$$\ddot{\mathbf{r}}_{4d} = \begin{bmatrix} \ddot{r}_{4yd} \\ \ddot{r}_{4zd} \end{bmatrix} = \begin{bmatrix} -0.2 \left(\frac{2\pi}{T_1}\right)^2 \sin\left(\frac{2\pi}{T_1}t\right) \\ 0 \end{bmatrix} \quad (32)$$

$${}^1\ddot{\mathbf{r}}_{2d} = \begin{bmatrix} \ddot{r}_{2yd} \\ \ddot{r}_{2zd} \end{bmatrix} = \begin{bmatrix} -0.2 \left(\frac{2\pi}{T_2}\right)^2 \sin\left(\frac{2\pi}{T_2}t\right) \\ 0 \end{bmatrix}$$

where $T_1 = 2.0$ s and $T_2 = 3.0$ s are constant, and the velocity and position of the hand are given as a periodic trajectory and are satisfied when $t = 0$. The torque for the reconfiguration of the second link is given as ${}^1\mathbf{l} = {}^1\Lambda_2^+ \Delta^1 \ddot{\mathbf{r}}_{2d}$, where $\Delta^1 \ddot{\mathbf{r}}_{2d}$ is calculated from Eqs. (15) and (16). Based on the abovementioned methodology, $\ddot{\mathbf{r}}_{4d}$ is calculated from Eq. (7). The input torque $\boldsymbol{\tau}$ is then calculated from Eq. (31). Finally, the motion of the manipulator is calculated from Eq. (1). Even if the acceleration of the middle link is generated ideally, the velocity and position still contain an offset error under the condition that the initial position or velocity differs from the desired initial state. To tackle this issue of the initial conditions, the desired acceleration was modified using linear feedback from the velocity and position as

$${}^1\ddot{\mathbf{r}}_{2d}^* = {}^1\ddot{\mathbf{r}}_{2d} + \mathbf{H}_v(\dot{\mathbf{r}}_{2d} - \dot{\mathbf{r}}_2) + \mathbf{H}_p(\mathbf{r}_{2d} - \mathbf{r}_2) \quad (33)$$

where \mathbf{H}_v and \mathbf{H}_p are the positive definite diagonal matrices. This feedback control equation is based on the ‘‘local optimization’’

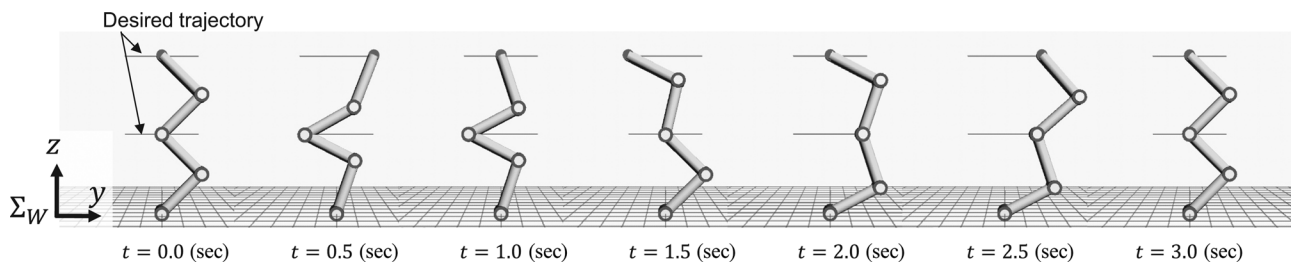


Fig. 11 Desired trajectory of hand and tip of second link

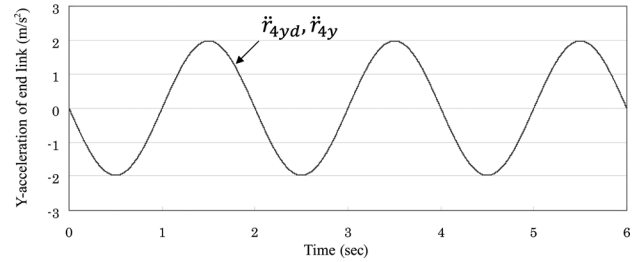


Fig. 12 Performance of hand acceleration

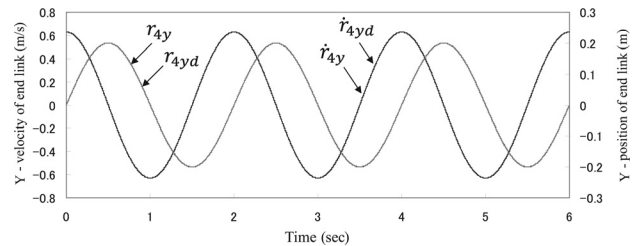


Fig. 13 Performance of hand velocity and position

criterion given in Ref. [21]. In this simulation, $\mathbf{H}_v = \text{diag}[30, 30]$ and $\mathbf{H}_p = \text{diag}[100, 100]$ are adopted. From Eq. (16), $\Delta^1 \ddot{\mathbf{r}}_{2d} = {}^1\ddot{\mathbf{r}}_{2d} - {}^1\ddot{\mathbf{r}}_{2d}$ is true. Therefore, in Eq. (19), the torque ${}^1\mathbf{l}$ is given to simulate the shape reconfiguration under the condition that $\Delta^1 \ddot{\mathbf{r}}_{2d}$ is calculated by replacing ${}^1\ddot{\mathbf{r}}_{2d}$ in Eq. (16) with ${}^1\ddot{\mathbf{r}}_{2d}^*$. In this case, $\text{rank}({}^1\Lambda_2) = 2$, and $(\mathbf{I}_n - {}^1\Lambda_2^+ {}^1\Lambda_2)$ is thus a null matrix. In this simulation, \mathbf{r}_{2d} and $\dot{\mathbf{r}}_{2d}$ are obtained by the numerical integration of $\ddot{\mathbf{r}}_{2d}$. The simulation results are shown in Figs. 11–15 as follows. The appearance of the manipulator during the simulation is illustrated in Fig. 11. The acceleration of the hand in the y -direction is shown in Fig. 12, and its velocity and position are shown in Fig. 13. The acceleration of the link is shown in Fig. 14, and its velocity and position are shown in Fig. 15.

The acceleration of the hand agreed very well with the desired acceleration, and the tracking performance of the velocity and position of the hand was realized. In addition, the generated acceleration $\ddot{\mathbf{r}}_2$ of the second link was in good agreement with the desired acceleration $\ddot{\mathbf{r}}_{2d}$, despite the fact that the $\ddot{\mathbf{r}}_2$ is affected by the hand task $\ddot{\mathbf{r}}_{4d}$. Thus, these simulations confirmed that the proposed algorithm was able to compensate for the errors of both the velocity and position of the second link, where $\ddot{\mathbf{r}}_{2d}^*$ was adopted as the provisional desired acceleration to achieve $\ddot{\mathbf{r}}_{2d}$.

4 Discussion

This section discusses the possibility of adapting DRM to other robot systems with a focus on humanoid robots because they also

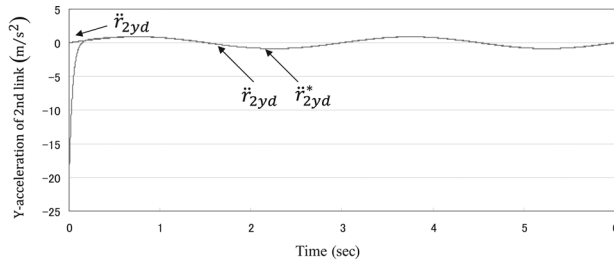


Fig. 14 Performance of acceleration of second link

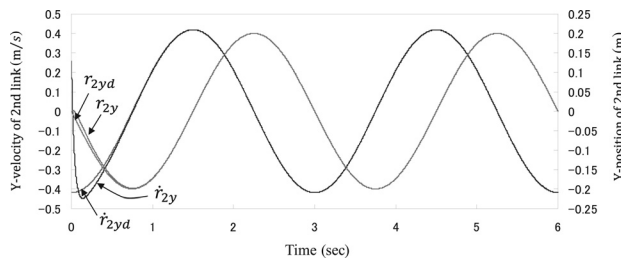


Fig. 15 Performance of velocity and position of second link

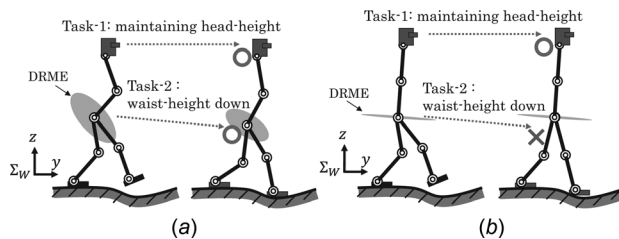


Fig. 16 Humanoid robot walking on uneven ground. (a) Non-singular configuration: redundant ability to accelerate the waist position while maintaining head height and placing the foot on the uneven ground. (b) Partially singular configuration (from waist to head): cannot afford to maintain the current head height while placing the foot on the ground. This inability is demonstrated by the DRME of waist having narrow width.

exhibit redundancy when executing walking tasks [14]. Drawing parallels between the abovementioned four-link manipulator system and a humanoid robot, the head and waist of a humanoid robot can be considered analogous to the hand and second link of the manipulator, respectively, though there remain differences between the fixed conditions of the base points of the two robots. When DRM is adapted to a humanoid robot, the position of the waist can be evaluated as follows. This discussion is only an overview, and deeper analysis remains an issue for future work.

Considering a situation in which a humanoid robot walks on uneven ground, as shown in Fig. 16, the robot is executing two tasks: maintaining the height of its head (task 1) and lowering the height of its waist (task 2). These tasks assume that the robot's face should be directed toward a certain object while walking on the uneven ground. In Fig. 16(a), there is allowance for the z -acceleration of the waist, allowing some leeway for the robot to simultaneously achieve tasks 1 and 2. Conversely, in Fig. 16(b), there is little allowance for the z -acceleration of the waist; in this case, task 1 can be achieved, but task 2 cannot. Thus, because maintaining a constant head height is the primary task, the height of waist cannot be kept constant. This can be also understood

based on the fact that the DRME of the waist degenerated to a disk in Fig. 16(b). This means that DRM can be applied as a measure of evaluating the capability of a humanoid robot to multitask while walking.

5 Conclusion

In this paper, we explained the concept of DRM for redundant manipulator, which was originally proposed in Refs. [14] and [17] for bipedal robot. The DRM expresses the ease with which the acceleration of the middle link of a redundant manipulator can be generated by a torque that has no effect on the task of the hand. We analyzed the dynamics of robotic manipulator by DRM in the case of a hand oscillatory acceleration task being given as the primary task.

Then, we revealed the difference between the DRM ellipsoid and the RM ellipsoid, emphasizing that the kinematical and dynamical manipulabilities differ and should be discussed separately depending on the hand and intermediate link tasks. Furthermore, this paper reveals that the optimal configurations of the manipulator evaluated by the DRM and RM ellipsoids are different, which suggests that whether DRM or RM should be used to optimize the entire configuration of the manipulator hinges on what type of task is required for the hand and intermediate links. The effectiveness of the index based on DRM was confirmed through simulations in which the index was adopted to a four-link manipulator.

References

- Asada, H., 1983, "A Geometrical Representation of Manipulator Dynamics and Its Application to Arm Design," *ASME J. Dyn. Syst. Meas. Control*, **105**(3), pp. 131–135.
- Yoshikawa, T., 1985, "Manipulability of Robotic Mechanisms," *Int. J. Rob. Res.*, **4**(2), pp. 3–9.
- Yoshikawa, T., 1985, "Dynamic Manipulability of Robot Manipulators," *IEEE International Conference on Robotics and Automation (ICRA)*, St. Louis, MO, Mar. 25–28, pp. 1033–1038.
- Koepe, R., and Yoshikawa, T., 1997, "Dynamic Manipulability Analysis of Compliant Motion," *IEEE/RJSJ International Conference on Intelligent Robots and Systems (IROS '97)*, Grenoble, France, Sept. 7–11, Vol. 3, pp. 1472–1478.
- Chinacchio, P., 2000, "New Dynamic Manipulability Ellipsoid for Redundant Manipulators," *Robotica*, **18**(4), pp. 381–387.
- Kurazume, R., and Hasagawa, T., 2004, "Impedance Matching for a Serial Link Manipulator," *IEEE International Conference on Robotics and Automation (ICRA '04)*, New Orleans, LA, Apr. 26–May 1, pp. 4802–4808.
- Yoshida, K., Hata, N., Oh, S., and Hori, Y., 2009, "Extended Manipulability Measure and Application for Robot Arm Equipped With Bi-Articular Driving Mechanism," *35th Annual Conference of the IEEE Industrial Electronics Society (IECON '09)*, Porto, Portugal, Nov. 3–5, pp. 3083–3088.
- Naksuk, N., and Lee, C. S. G., 2006, "Zero Moment Point Manipulability Ellipsoid," *IEEE International Conference on Robotics and Automation (ICRA 2006)*, Orlando, FL, May 15–19, pp. 1970–1975.
- Yim, M., Zhang, Y., Roufas, K., Duff, D., and Eldershaw, C., 2002, "Connecting and Disconnecting for Chain Self-Reconfiguration With PolyBot," *IEEE/ASME Trans. Mechatronics*, **7**(4), pp. 442–451.
- Mohamed, M. G., and Gosselin, C. M., 2005, "Design and Analysis of Kinetically Redundant Parallel Manipulators With Configurable Platforms," *IEEE Trans. Rob.*, **21**(3), pp. 277–287.
- Murata, S., Yoshida, E., Kamimura, A., Kurokawa, H., Tomita, K., and Kokaji, S., 2002, "M-TRAN: Self-Reconfigurable Modular Robotic System," *IEEE/ASME Trans. Mechatronics*, **7**(4), pp. 431–441.
- Minami, M., Zhang, T., Yu, F., Nakamura, Y., Yasukura, O., Song, W., Yanou, A., and Deng, M., 2010, "Reconfiguration Manipulability Analyses for Redundant Robots in View of Structure and Shape," *International Conference of SCIS and ISIS*, Okayama, Japan, Dec. 8–12, pp. 971–976.
- Zhang, T., Minami, M., Yasukura, O., and Song, W., 2013, "Reconfiguration Manipulability Analyses for Redundant Robots," *ASME J. Mech. Rob.*, **5**(4), pp. 1–16.
- Kobayashi, K., Minami, M., Yanou, A., and Maeda, T., 2013, "Dynamic Reconfiguration Manipulability Analyses of Humanoid Bipedal Walking," *2013 IEEE International Conference on Robotics and Automation (ICRA2013)*, Karlsruhe, Germany, May 6–10, pp. 4764–4769.
- Maciejewski, A. A., and Klein, C. A., 1985, "Obstacle Avoidance for Kinetically Redundant Manipulators in Dynamically Varying Environments," *Int. J. Rob. Res.*, **4**(3), pp. 109–117.

- [16] Iagnemma, K., Rzepniewski, A., Dubowsky, S., Pirjanian, P., Huntsberger, T., and Schenker, P., 2000, "Mobile Robot Kinematic Reconfigurability for Rough-Terrain," *Proc. SPIE*, **4196**, p. 413.
- [17] Kobayashi, K., Minami, M., Yanou, A., and Maeda, T., 2012, "Dynamic Reconfiguration Manipulability Analyses of Redundant Robot and Humanoid Walking," 2012 IEEE/SICE International Symposium on System Integration (*SI 2012*), Fukuoka, Japan, Dec. 16–18, pp. 73–78.
- [18] Liegeois, A., 1977, "Automatic Supervisory Control of the Configuration and Behavior of Multibody Mechanisms," *IEEE Trans. Syst. Man Cybern.*, **7**(12), pp. 868–871.
- [19] Hewit, J. R., and Burdess, J. S., 1981, "Fast Dynamic Decoupled Control for Robotics, Using Active Force Control," *Mech. Mach. Theory*, **16**(5), pp. 535–542.
- [20] Galicki, M., 1991, "A Closed Solution to the Inverse Kinematics of Redundant Manipulators," *Mech. Mach. Theory*, **26**(2), pp. 221–226.
- [21] Siciliano, B., and Khatib, O., 2008, *Springer Handbook of Robotics*, Springer-Verlag, Berlin, Chap. 11.
- [22] Minami, M., Naitoh, Y., and Asakura, T., 1999, "Avoidance Manipulability for Redundant Manipulators," *J. Rob. Soc. Jpn.*, **17**(6), pp. 887–895 (in Japanese).